

## Phase Separation Kinetics of a Polymer Blend Modified by Random and Block Copolymer Additives

Bethany Barham, Kari Fosser, Gretchen Voge, and Dean Waldow\*

*Department of Chemistry, Pacific Lutheran University, Tacoma, Washington 98447*

Adel Halasa

*Corporate Research Division, The Goodyear Tire and Rubber Company, 142 Goodyear Blvd., Akron, Ohio 44305*

*Received December 30, 1999*

**ABSTRACT:** The phase separation behavior of polymer blends modified by copolymer additives has been studied using light scattering techniques. Block and random copolymers with equal styrene and butadiene content as well as a random copolymer with unequal monomer composition were used as additives at a concentration of 2.5% (w/w). The symmetric additives lowered the phase boundary with increasing concentration while the asymmetric additive destabilized the phase boundary. The data demonstrate a slowing of the kinetics with the addition of any of the copolymers. In comparison to the binary blend, droplet sizes in the early stage were smaller with added symmetric block copolymer and larger with added asymmetric random copolymer. Scaling analysis of the intermediate stage kinetics showed some deviations relative to binary scaling results. Deviations from Porod's law indicate that modifications to the interfacial boundary are most notable for the asymmetric random copolymer. Self-similarity was seen to hold for all of the systems.

### Introduction

The development of a new polymer blend is generally driven by the need to design a substance with properties not in a current single material. The blending of common polymers to produce new substances has become very common and often effective in this endeavor.<sup>1–3</sup> However, the realities of low miscibility for polymer blends have led to extensive research into the thermodynamic and kinetic properties of polymer blends.<sup>4–12</sup> A common method to enhance poor miscibility is to add a third component to a blend that will have a favorable interaction with the precursor polymers. This third component, often termed a compatibilizer, is designed with the hope it will favorably affect the blend system by potentially changing a miscibility window, strengthening phase-separated domains, or affecting the kinetics of phase separation, thus causing a change in the phase-separated morphology. A logical candidate for an additive is an A–B copolymer containing the monomers of the polymers, which make up the blend. These types of additives are still numerous given the variety of possible copolymer structures. It is likely that different copolymers will have distinct differences in their effect on a polymer blend.

The structure of a copolymer additive is an important consideration in blending polymers. Research by Kramer and co-workers<sup>13,14</sup> has demonstrated that a long symmetric random copolymer can lead to stronger interfaces than a long diblock copolymer or an asymmetric random copolymer. They additionally suggested that block copolymers might be more effective at lowering interfacial tension while random copolymers may be more effective at reinforcing interfacial strength. Noolandi and Shi,<sup>15</sup> on the other hand, suggest that, for melt processing, random copolymers lack sufficient

driving force to localize at an interfacial boundary compared with a similar concentration of block copolymer. Balasz<sup>16–18</sup> and co-workers have studied miscibility and interfacial tension as a function of copolymer structure with theoretical methods. From their work, it was found that blend miscibility was a strong function of copolymer structure and that from a thermodynamic perspective block copolymers were not necessarily the best compatibilizers. In comparing different linear and branched copolymers, interfacial tension was lowered most effectively by diblock copolymers while studies with longer comb or random copolymers were more effective than short diblock copolymers. Dadmun<sup>19,20</sup> has also studied blend properties as a function of copolymer structure using Monte Carlo simulations on a square lattice. This work found that all classes of copolymers migrated to the interface while sequence distributions different from that of a purely random copolymer were more promising in strengthening interfaces. Dadmun also noted that most copolymers, which are not block or alternating, are often referred to as random and are not likely equivalent to a theoretical random copolymer. Last, Dadmun and Waldow<sup>21</sup> have also studied the effect a copolymer has on the critical properties of a polymer mixture. Added copolymer changed the critical properties (namely correlation length) from an Ising-like system to one that is in qualitative agreement with Fisher renormalization.

There are relatively few experimental studies reported in the literature pertaining to thermodynamics and more specifically the kinetics of phase separation for binary blends with additives. Most of these studies have focused on the addition of a symmetric A–B block copolymer added to a binary blend of polymers A and B. Rigby, Lin, and Roe<sup>22</sup> have studied the phase boundary modifications by both random and block copolymers. The low molecular weight random copolymers proved more effective at lowering the phase boundary than did

\* To whom correspondence should be addressed.

either a high molecular weight random copolymer or a similar molecular weight diblock copolymer. Roe and co-workers<sup>23,24</sup> have also studied a polystyrene–polybutadiene system with an added diblock component. In both microscopy and light scattering, the results showed that the rate of phase separation was slowed with the addition of diblock copolymer. The effect was pronounced with increase in either the concentration or molecular weight and was explained in terms of reduction of interfacial tension by the diblock copolymer. The light scattering data were for temperature jumps to a constant final temperature, and therefore the quench depths were not equivalent for each blend. In a related system, Han and co-workers<sup>25</sup> studied a polystyrene–polybutadiene blend also with added diblock copolymer. This work also showed a reduction in growth rate as well as a reduction in the size scale of the phase-separated microstructure with added diblock copolymer. In another system, Hashimoto and Izumitani<sup>26</sup> studied the phase separation kinetics of polybutadiene and poly(styrene-*ran*-butadiene) with added diblock copolymer at a variety of quench depths. This study also demonstrated a reduction in growth rate with increasing block copolymer concentration, which was only partially attributed to larger molecular weight of the copolymer as compared to the blend polymers. Takenaka and Hashimoto<sup>27</sup> have reported results from a theoretical study of the early-stage spinodal decomposition in a binary blend compatibilized by a random copolymer. They extended the Cahn–Hilliard–Cook<sup>28</sup> theory to apply to this ternary system. They found that for the early stages of separation there is much in common with the binary blend.

Given the importance of additive structure on the thermodynamic interaction and changes to interfacial tension, it is important to conduct experiments investigating the effect that different copolymers have on the phase separation process for polymer blends. Using knowledge from these types of experiments, one can more effectively tailor compatibilizers to meet specific needs. The goal of this study is to better understand the role that an additive's structure has on equilibrium properties and on the kinetics of phase separation for binary blend systems. Blends of polystyrene and polybutadiene modified by various additives are investigated. The additives studied are symmetric and asymmetric random copolymers as well as a symmetric block copolymer. Changes in the cloud point with increasing additive concentration are presented along with phase separation kinetics at a concentration of 2.5 % (w/w) for the various additives. The kinetics data presented here are in the early and intermediate stages of phase separation at a variety of shallow quench depths.

## Experimental Section

**Materials and Preparation.** The molecular characteristics of the polymers used in this work are summarized in Table 1. The PS and PB homopolymers and the three copolymers were synthesized at the Goodyear Tire and Rubber Co. by anionic techniques. The samples were purified by dissolving in solvent (PS: benzene; PB and SBR2080: hexane; and SBB5050 and SBR5050: toluene) and then filtered first through a fritted glass filter and second through a Teflon membrane filter (Bio-Rad, 0.45  $\mu\text{m}$ ). The solvents were removed by freeze-drying for the PS system. The others were evaporated to constant weight in a vacuum oven at a temperature on the order of 60 °C or less.

The blend samples were weighed directly in microscale conical vials in the bulk state. The antioxidant, Goodyear

Table 1. Polymer Sample Characteristics

sample code	$M_w \times 10^3$	$M_w/M_n$	content (%) <sup>e</sup>		microstructure (%) <sup>f</sup>	
			$w_{\text{PS}}$	$w_{\text{PB}}$	cis and trans	vinyl
PS <sup>a</sup>	1.94	1.19	100	0	n/a	n/a
PB <sup>b</sup>	2.98	1.08	0	100	92	8
SBR2080 <sup>c</sup>	17	1.1	20	80	86	14
SBR5050 <sup>c</sup>	68.2	3.7	51	49	73	27
SBB5050 <sup>d</sup>	27.7	1.06	50	50	90	10

<sup>a</sup> Poly(styrene). <sup>b</sup> Poly(butadiene). <sup>c</sup> Poly(styrene-*ran*-butadiene). <sup>d</sup> Poly(styrene-*block*-butadiene). <sup>e</sup> Weight percent of component in copolymer. <sup>f</sup> Microstructure of butadiene portion of copolymer.

Wingstay #29, was used at concentrations on the order of 0.1% (w/w) or less. The binary and ternary blend systems were all prepared such that the PS and PB homopolymers were at a constant mass fraction of 0.75 with respect to PS. They were heated in a vacuum oven to a temperature above the sample glass transition temperature, allowed to melt, and mechanically mixed, and then the oven was evacuated. The samples were periodically mixed over a period of 4–6 h. The resulting blends were found to be homogeneous through both visual examination of the phase separation during the cooling of the vials and consistent phase boundary measurements for multiple samples with identical composition. Additionally, this mechanical mixing method was found to produce blends with more consistent phase boundary temperatures than blends prepared by evaporation from a good solvent.

For both cloud point measurements and temperature jump light scattering measurements, the samples were prepared by placing 1–2 drops of the blend sample (heated above the phase boundary) on one of the two quartz flats used in the cell. The blend sample would rapidly quench in temperature and solidify. A Teflon spacer (125  $\mu\text{m}$ ) was used between the two quartz flats to both maintain the sample path length and seal the sample cell. The sample cell was heated until the blend softened whereby the cell was compressed to seal the system.

A Bausch-Lomb Abbe refractometer was used to measure the index of refraction of all of the polymer systems used except for PS, for which values were taken from Krause and Lu.<sup>29</sup> The measurements were made in the temperature range from room temperature to 90 °C. The data were then extrapolated linearly to the experiment temperature needed. The index of refraction of a blend sample was calculated from the individual indices of refraction.

**Cloud Point Measurements.** To determine the phase diagrams of the systems studied, a cloud point instrument was constructed. This instrument consisted of a temperature-controlled ( $\pm 0.1$  °C, PID controller) sample holder and was designed to allow a HeNe laser ( $\lambda = 632.8$  nm, 2 mW, Melles Griot) beam to be directed through the sample. The transmitted intensity as well as the light scattered at a fixed angle ( $\sim 25^\circ$ ) was measured using amplified photodiodes. Both the monitoring of the intensity of light reaching both detectors and the control of the sample temperature were accomplished using a computer interface. Generally, the sample under investigation was allowed to equilibrate for 30–60 min in the one-phase region about 30°–40° away from the phase boundary. The temperature of the sample was then ramped at a rate of 0.5 °C/min toward the two-phase region. The onset of a phase separation was considered the point at which the transmitted or scattered intensity first deviated from the value in the one-phase region.

**Temperature Jump Light Scattering.** A light scattering instrument (see Figure 1) was constructed to measure scattering over a wide array of angles and with good temporal resolution (30 ms). This system was designed along the lines of Sato et al.<sup>30</sup> and employed corrections for scattered light following Stein and Keane.<sup>31</sup> The light source was a HeNe laser ( $\lambda = 632.8$  nm, 10 mW, Melles Griot) polarized vertically. The detector was a 1024 photodiode array (Princeton Applied Research, model 1453A) and was interfaced to a model 1471 Princeton Applied Research controller. The sample holder was

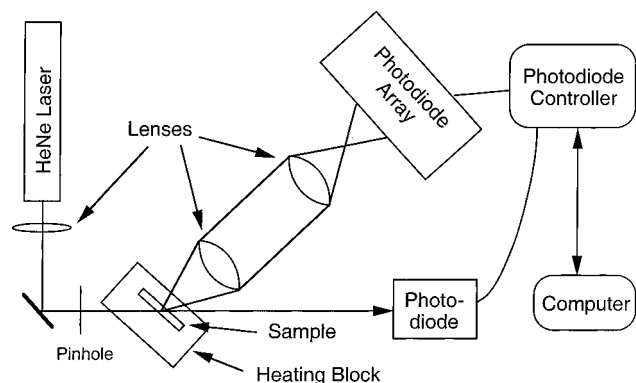


**Figure 1.** Schematic of the temperature jump wide-angle light scattering instrument is shown. The initial temperature controlled sample block is not included.

mounted on a rotary table with the axis of rotation positioned at the scattering center. The scattered light was collimated with a low focal length lens and imaged on the detector with an identical lens. The working angular range for this system is on the order of  $65^\circ$ . The rotary table's angle can be easily changed to accommodate the angular needs of a particular experimental system. The sample holder is temperature controlled via a PID controller with proportional heating and has an accuracy of  $\pm 0.03^\circ\text{C}$ . An additional duplicate sample holder and temperature controller were used where the sample was maintained until the temperature jump was initiated. The transmitted laser intensity (for turbidity corrections) was monitored via a separate amplified photodiode and measured by the controller concurrently with the photodiode array. The sensitivity of each photodiode in the array was calibrated using an aqueous methylene blue solution ( $1 \times 10^{-5}\text{ M}$ ). The calibration of the angle or scattering vector,  $q = (4\pi/\lambda) \sin(\theta/2)$ , for each pixel of the photodiode array was accomplished by a transmission grating. The temperature controllers for the two sample chambers and the photodiode controller were interfaced to a computer for experiment control and data acquisition.

Samples were heated in the preparatory block to sufficiently above their respective phase boundaries and allowed to equilibrate at least 30 min before a temperature jump. The temperature jump was conducted by moving a sample to the working sample block in the scattering instrument. The time dependence of the temperature change was exponential with a time constant ( $1/e$  time) for the sample to reach the new temperature of  $38 \pm 2\text{ s}$ , and 3 times this time constant was designated as zero time for the phase separation process.

## Results and Discussion

**Equilibrium Thermodynamics.** A plot of the cloud point temperature versus copolymer weight fraction is shown in Figure 2 for the three copolymers used in this study. The composition of the binary blend is held constant at a ratio of 3:1 for PS relative to PB and is slightly away from the critical composition though only spinodal decomposition kinetics have been observed. It was seen that with both SBB5050 and SBR5050 the blend was stabilized by the addition of copolymer with the block copolymer being the most effective at shifting the phase boundary. To the contrary, the asymmetric random copolymer, SBR2080, destabilized the phase boundary, thus shifting the cloud point to higher temperatures with increasing copolymer concentration. All three copolymers affected the phase separation temperature in a linear fashion, up to the highest concentration measured. The SBR2080 data were prepared with a different batch of PB that simply resulted in a slightly lower phase boundary for all samples made with that PB. The important considerations are the deviations

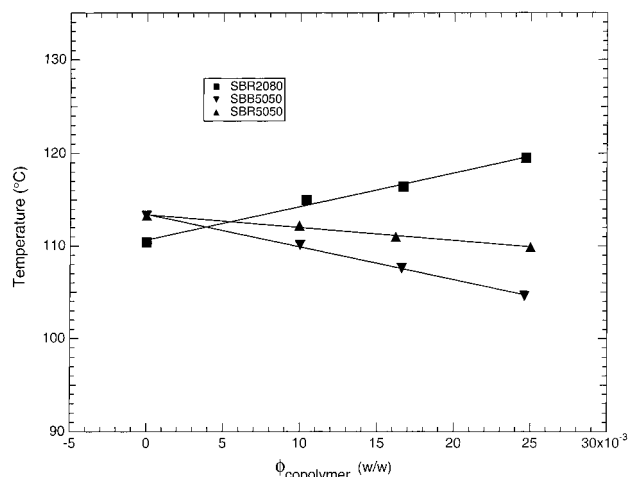


**Figure 2.** Plot of cloud point temperature versus copolymer additive weight fraction (w/w). The lines are linear least-squares fits to the data.

from the binary blend caused by the addition of copolymer, and the minimal difference in the two batches is not significant.

The lowering of the phase boundary with added symmetric block copolymer in this study is consistent with other measurements in the literature where the studies employed similar polymer systems. Roe and Kuo<sup>32</sup> found that an added symmetric diblock of styrene and butadiene with increasing copolymer content (which was similar to the one used in this study) lowered the cloud point. This effect on the cloud point was less pronounced than the data in this study. Han and co-workers<sup>25,33</sup> also studied a related system (higher molecular weight PS and lower molecular weight PB) and found that the cloud point had a similar behavior while the dependence on copolymer content was weaker.

Less attention in the literature has been given to the effect random copolymer structures have on the phase boundary than the effect of block copolymers. Rigby et al.<sup>22</sup> studied the effect that three different random copolymers had on the cloud point of a binary PS–PB blend. The copolymers they studied were close to equal composition in the two monomers. Two of the random copolymers were of lower molecular weight with one of the two prepared anionically and the other prepared via free radical methods. The third random copolymer had a weight-average molecular weight on the order of 300 000 Da and was about a factor of 10 larger than the other two random copolymers. The polydispersity of this high molecular weight sample was not quoted, but the sample was believed to be prepared via free radical techniques. They found almost identical behavior for the two lower molecular weight copolymers where they were fairly effective at lowering the cloud point. However, the larger molecular weight and presumably polydisperse random copolymer was ineffective at low concentrations and only started to have an appreciable effect on cloud point temperatures at volume fractions greater than 0.1. They attribute this to the higher molecular weight, which is argued induces a three-phase separation. The molecular weight of the symmetric random copolymer (SBR5050) used in this study was in between the molecular weights used in their system and was polydisperse. The results for this copolymer on lowering the cloud point were not as effective as Rigby's lower molecular weight random copolymer samples and



more effective than their high molecular weight sample. This result is consistent with Rigby's results if the polydispersity of the SBR5050 sample is considered crudely to have higher and lower molecular weight portions. The lower molecular weight portion is much more effective at compatibilization though is not a majority component while the higher molecular weight portion is not an effective compatibilizer at low concentrations. The combination of these two portions would lead to a smaller effect on the phase boundary because of a lower effective concentration of the lower molecular weight component at a given copolymer concentration. Last, the SBR5050 sample is not believed to be in a three-phase region given the lower molecular weight and low concentration.

Dudowicz and co-workers<sup>34</sup> have presented theoretical work investigating the phase boundary properties of binary polymer blends modified by diblock copolymer additives where copolymer composition and structure were varied. Lattice cluster theory calculations were used to model the three different ternary blends. One conclusion pertinent to this report was that when adding a diblock copolymer the phase boundary could be stabilized or destabilized by adjusting the composition of the block copolymer. The cloud point data for SBB5050 are consistent with their result that a symmetric block copolymer lowers the phase boundary compared to the binary blend. The authors also describe the Timmermans<sup>35–37</sup> mixing rule, which states that an additive which is soluble in both precursors of the blend will tend to stabilize the system while if the additive is preferentially soluble in one component the system will be destabilized. This work's results show that the blend is destabilized with addition of SBR2080. This additive has a strong preferential solubility for PB where it is soluble at all compositions while for PS the additive has a cloud point slightly above 100 °C at low concentrations with PS. This preferential solubility of the additive and the destabilization are consistent with Timmermans' rule as well as Dudowicz's modeling results for asymmetric block copolymers.

**Phase Separation Kinetics.** Temperature jump light scattering measurements were conducted on the binary PS/PB blend and three other PS/PB blends, each modified by a different copolymer listed in Table 1 at a concentration of 2.5% (w/w). The time evolution of these data was measured so that the kinetics of phase separation could be studied at a series of shallow quench depths below the phase boundary. Two examples of the light scattering data are presented. Figure 3 shows the scattering intensity as a function of scattering vector,  $q$ , for the binary PS/PB blend. Figure 4 also shows the scattering intensity (same arbitrary units as in Figure 3) as a function of scattering vector for the same binary blend modified by the asymmetric copolymer, SBR2080, at 2.5% (w/w). For both figures, the quench depth below the phase boundary was one degree, and the insets of the figures list the time after the temperature jump for each curve. The solid circles indicate the estimated position of the scattering vector at the maximum scattering intensity. As expected for the two data sets, the spinodal peak grows in intensity and moves to smaller scattering vectors as the transition to the two-phase state progresses. The data for Figure 4 show much slower kinetics of phase separation than the data in Figure 3. The addition of the asymmetric copolymer influenced more than the temperature of the phase

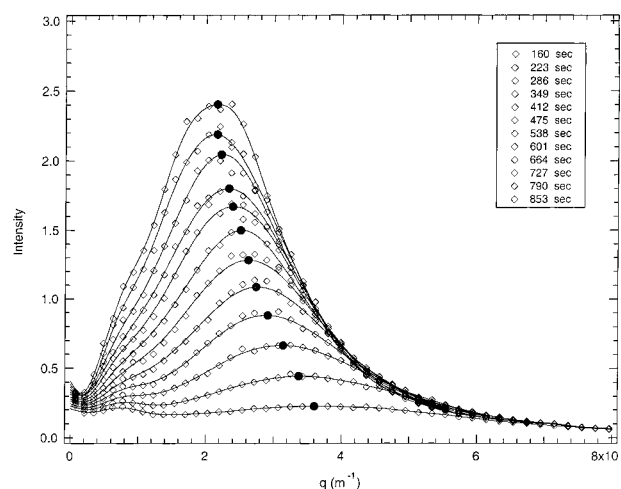


**Figure 3.** Plot of scattering intensity versus wave vector ( $\text{m}^{-1}$ ) for various times after a temperature jump for a binary PS/PB blend. The lines running through the points are a visual aid. The filled circles represent the scattering maximum for each curve.

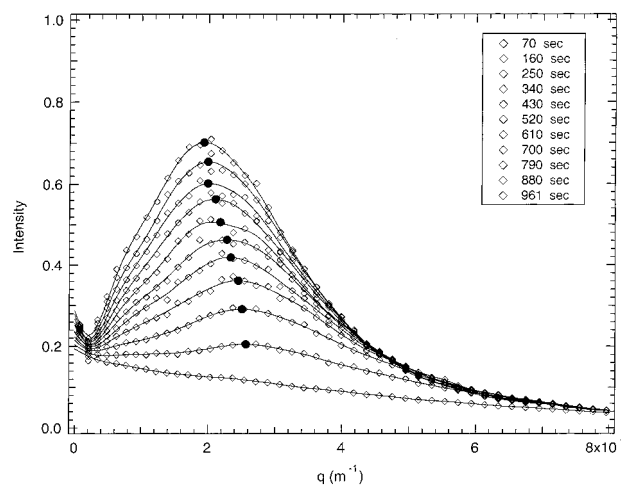


**Figure 4.** Plot of scattering intensity versus wave vector ( $\text{m}^{-1}$ ) for various times after a temperature jump for a binary PS/PB blend with added SBR2080. The lines running through the points are a visual aid. The filled circles represent the scattering maximum for each curve. The intensity axis is in the same arbitrary unit scale as in Figure 3.

boundary. The copolymer also significantly slowed the rate of the separation process for this additive system.

The kinetics of the separation seen in Figures 3 and 4 are so fast that analysis of the early stage behavior (Cahn–Hilliard–Cook region) was not practical. A different method was needed to compare the rate of phase separation for the different blend systems instead of using apparent diffusion coefficients. Hence, a linear estimation of the rate of growth of the maximum intensities was used as a measure. The rate of growth was also calculated using integrated intensities, and the results were the same. Figure 5 presents this rate of growth for each blend system at a variety of quench depths. The rate of phase separation was slower in all modified blends as compared to the binary blend. The blends with the block copolymer (SBB5050) and the asymmetric random copolymer (SBR2080) were more effective at retarding the phase separation than the symmetric random copolymer (SBR5050). The only exception was at the deepest quench for the SBR2080, where the rate was similar to that of the SBR5050. Last,

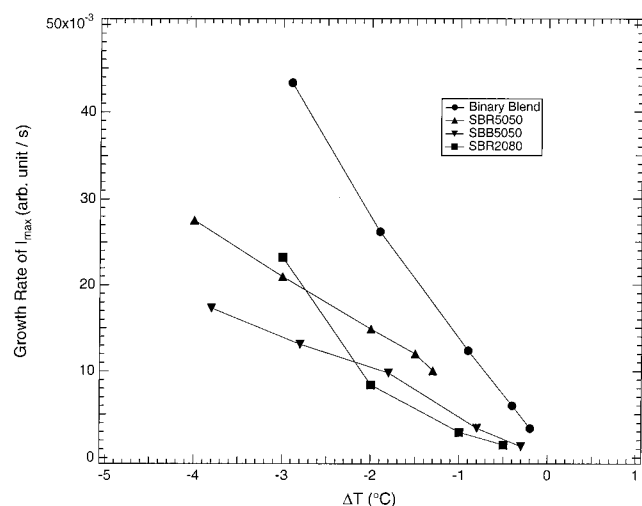


**Figure 5.** Plot of the growth rate of the droplets as a function of quench depth into the two-phase region for the binary blend and the binary blend modified by three different copolymer additives. The inset indicates the data set identification is used in the following figures.

the effective slowing of the rate of phase separation weakens in the SBR2080 sample for the deepest temperature quench. This effect is not understood, and future data at deeper quenches and higher additive concentrations will be helpful in understanding this result.

This slowing of kinetics has been seen previously for diblock copolymer additives. Sung et al.<sup>25,33</sup> and Roe et al.<sup>23</sup> have seen similar behavior when PS/PB systems were modified by a PS/PB diblock copolymer at low concentrations. Hashimoto et al.<sup>26</sup> have also studied a blend system modified by a diblock of the two blend polymers where they noted the slowing of kinetics with increasing copolymer content. The slowing of phase separation kinetics is generally attributed to the copolymers migrating to the interface and thus lowering the interfacial tension. In turn, the driving force for separation is also reduced. The idea of the copolymers migrating to the interface is also seen with Monte Carlo simulations by Dadmun<sup>19,20</sup> where the various copolymers studied migrated to the interface. The argument regarding lower interfacial tension is also consistent with the fact that the phase boundary is lowered in these blends with added diblock content.

The most striking result from Figure 5 is that for all ternary blends the rate of phase separation is slowed regardless of the additive or quench depth. Therefore, even when the phase boundary of a blend system is *destabilized* as for the SBR2080 blend, the rate of phase separation is slowed. The slowing of the rate of phase separation for an additive system with an increase in the phase boundary temperature to our knowledge has not been reported in the literature. This result raises interesting questions regarding the effect of copolymer on the bulk thermodynamics and the connection to interfacial modification. For example, (1) does this asymmetric copolymer migrate to the interface in a fashion similar to the symmetric additives? (2) If the copolymer does migrate to the interface, what is the effect on the interfacial tension, and how does that relate to the bulk thermodynamic observations?

Aside from the influence of the additives on the kinetics of the phase separation, there are also effects on the droplet size during the separation process. In

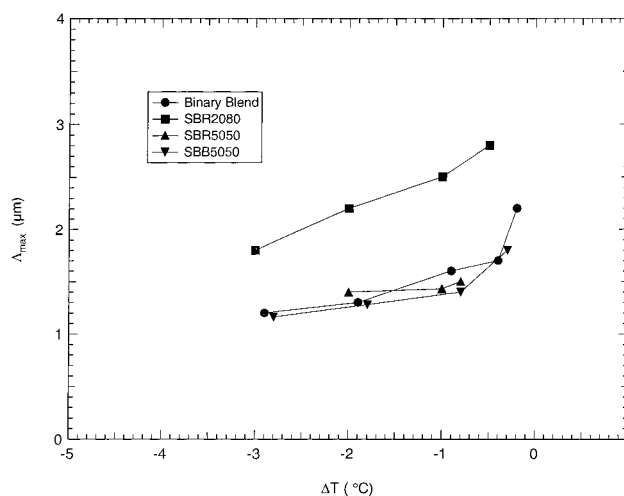


**Figure 6.** Plot of droplet size ( $\mu\text{m}$ ) as a function of quench depth for the same set of blends as in Figure 5. The droplet sizes are at the very beginning of the temperature jump.

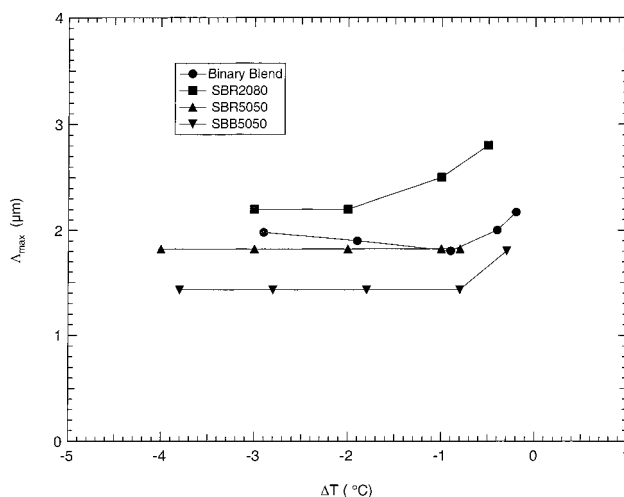


**Figure 7.** Plot of droplet size ( $\mu\text{m}$ ) plot as a function of quench depth for the same set of blends as in Figure 5. The droplet sizes are at 200 s into the temperature jump.

Figure 6,  $\Lambda_{\text{max}}$ , a real space descriptor of size ( $\Lambda_{\text{max}} = 2\pi/q_{\text{max}}$ ), is plotted for the various blend systems and quench depths at the onset of the phase separation. In the beginning stage of separation, the size of the phase separating domains is roughly equivalent for the binary blend as well as the ternary systems with symmetric copolymers. However, the initial size seen in the ternary blend with the SBR2080 additive is distinctly larger than the other three systems. This result is consistent with quench depth except that in all cases the initial size of the domains is reduced with increasing quench depth. Figure 7 shows the same type of plot as Figure 6 except at 200 s into the phase separation. As expected, the sizes of the domains increase as the phase separation process continues. However, there are notable distinctions. The binary blend and the blend with SBR5050 additive are essentially increasing in size together. In contrast, the SBB5050 blend is lagging behind the binary blend while the SBR2080 is still leading in domain size. The fact that the block copolymer modified system starts out at the same domain size as the binary blend indicates that domain growth is hindered by the block copolymer. This also corroborates the idea that the block copolymer does not halt growth at a point in time but rather impairs the blend's ability

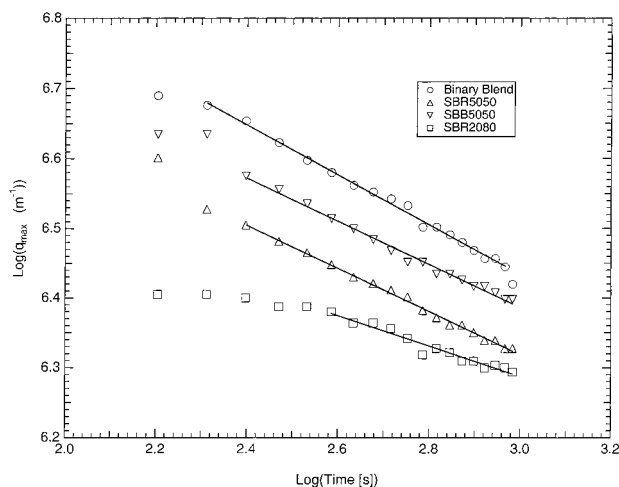


**Figure 8.** Scaling plot of the logarithm of the maximum wave vector ( $q_{\max}$ ) versus the logarithm of time in seconds. The lines are fits with the scaling values found in Table 2.

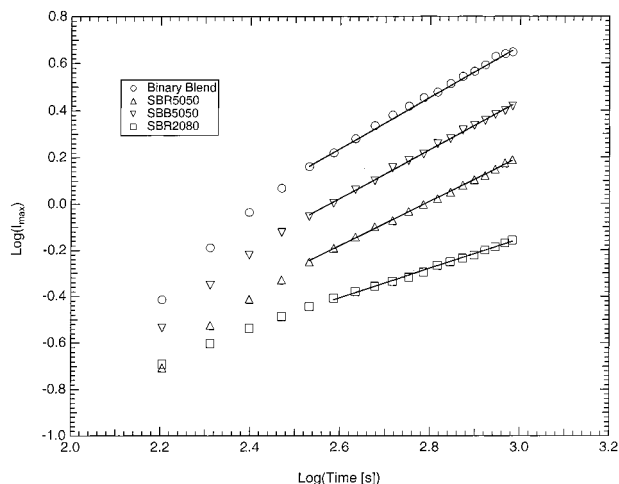


**Figure 9.** Scaling plot of the logarithm of the scattering intensity at maximum wave vector ( $I_{\max}$ ) versus the logarithm of time in seconds. The lines are fits with the scaling values also found in Table 2. The data have been arbitrarily shifted vertically for clarity.

to grow the domains. At times longer than 400 s, the quench depth was no longer a factor in the domain size. The domain size for each quench depth was equivalent at an equivalent time for each blend. However, the general differences between blends still holds where the blends with symmetric copolymer additives had smaller domain sizes than the binary blend. Furthermore, the blend with the asymmetric additive had larger domain sizes than the binary blend.

The intermediate and late stages of spinodal decomposition for binary blends can be described by a scaling relationship relating the peak intensity to time  $I_m \sim t^\beta$  as well as the wave vector at the peak intensity to time  $q_m \sim t^{-\alpha}$ . Experimental measurements have documented values of the scaling coefficients for binary blends in the intermediate stage as  $\alpha = 1/3$  and  $\beta = 1$  and in the late stage as  $\alpha = 1$  and  $\beta = 3$ .<sup>2,38,39</sup> Plots of the logarithm of  $q_m$  versus the logarithm of time are given in Figure 8 for the binary blend and the other three modified blends. The lines on this graph represent a measured slope for these two systems corresponding to the scaling coefficient,  $-\alpha$ . Additionally, Figure 9 presents the logarithm of  $I_m$  versus the logarithm of time for the binary blend and the other three modified blends. The

**Table 2. Scaling Results for a 1 °C Quench Depth**

blend	$\alpha$ ( $\pm 0.02$ )	$\beta$ ( $\pm 0.02$ )	$\alpha\beta$ ( $\pm 0.3$ )	$\gamma$ ( $\pm 0.4$ )
binary blend	0.35	1.09	3.1	3.9
SBB5050 <sup>a</sup>	0.29	1.0	3.5	3.2
SBR5050 <sup>a</sup>	0.31	0.97	3.1	4.0
SBR2080 <sup>a</sup>	0.23	0.64	2.8	2.7

<sup>a</sup> Binary blend with respective additive at 2.5% (w/w).

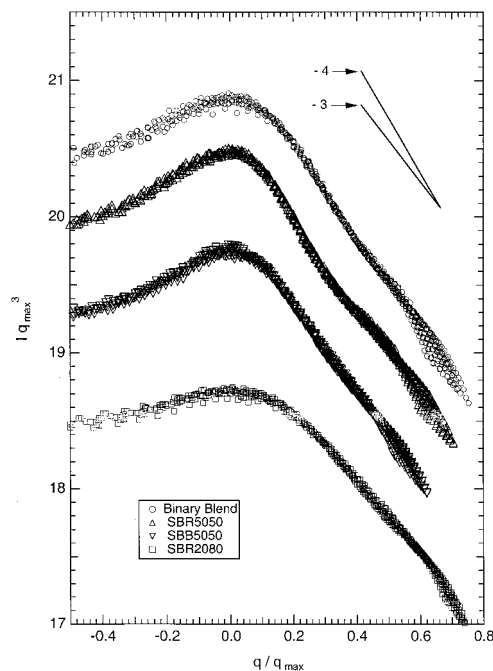


**Figure 10.** Self-similarity plots of the logarithm of the scattering intensity ( $I_{\max} q_{\max}^3$ ) times the cube of the scattering vector maximum versus the logarithm of the scattering vector maximum divided by the scattering vector maximum ( $q/q_{\max}$ ). The data sets are vertically offset for viewing. Two lines with slopes of  $-3$  and  $-4$  are included as a visual aid.

lines on this graph again represent a measured slope for these two systems corresponding to the scaling coefficient,  $\beta$ . The quench depth for the all data on these two plots is 1 °C. For the binary blend, the results ( $\alpha = 0.36$  and  $\beta = 1.09$ ) are in agreement with previous measurements. However, the results for the SBR2080 blend indicate significantly weaker scaling behavior with  $\alpha = 0.23$  and  $\beta = 0.63$ . The results for all four systems are given in Table 2. The scaling behavior for the SBR2080 blend deviates significantly from the binary behavior while the SBR5050 and SBB5050 system are, at best, marginally different. Last, it is clear that for the times accessed in these experiments only the intermediate stage of demixing is seen.

An important question arising from these studies relates to the location of the copolymer in the phase separation process. Does the copolymer migrate to the interface between the different composition domains, and how can this be measured? One way to attempt to gauge this is to analyze the sharpness between domains. This can be done by analyzing scaling behavior of the intensity dependence on wave vector, known as Porod's law<sup>40</sup> ( $I \sim q^{-\gamma}$ ). Porod's law states that if the boundary between two phases of material is sharp, then the value of the scaling coefficient  $\gamma$  will equal 4 for wave vectors greater than the maximum wave vector. If  $\gamma$  is less than four, the boundary between phases will not be sharp.<sup>41</sup> Figure 10 presents data for the binary blend and the other three modified blends all at the same quench



depth of one degree. The axes of the graph are intensity per domain volume at maximum intensity ( $Iq_m^3$ ) versus wave vector scaled to the wave vector at maximum intensity ( $q/q_m$ ). The slope of the data at  $q$  values greater than  $q/q_m = 1$  can be analyzed for the Porod scaling coefficient  $\gamma$ . These data can also be studied to assess self-similarity, which is addressed below. Two lines with slopes equal to  $-3$  and  $-4$  are also included in Figure 10 as a visual guide. Qualitatively, the binary blend data appear to be more similar to the  $-4$  slope line, while the SBR2080 blend data have a distinctly flatter slope. This suggests that the binary blend has a sharp interface while adding the SBR2080 copolymer to the blend makes the interface less defined. Table 2 lists the fits to the data for all four blend systems, again for equal quench depths of one degree. The binary blend and the blend modified by SBR5050 have sharp interfaces while the SBB5050 blend and the SBR2080 blend both have much less distinct interfaces. This argues that the SBB5050 and the SBR2080 most significantly modify the interface. The other aspect of Figure 10 is that of self-similarity. If light scattering data for one temperature jump experiment collapse into a universal curve, then the data can be said to be self-similar. In all cases for these experiments, the data do collapse onto a single curve once the spinodal decomposition has passed the early stage. All of the blend systems studied grew in very self-similar methods. The additives did not change the self-similarity. However, as seen in the scaling of the intensity versus wave vector, the additives did significantly influence the interfacial properties for the SBB5050 and SBR2080 blend systems.

Last, the large polydispersity and higher molecular weight of the SBR5050 sample were unique to the copolymers studied. This copolymer additive produced the least modifications to the binary polymer blend kinetics behavior of the additives studied. This is similar to the results in the equilibrium section where the SBR5050 had the least effect on the modification of the phase boundary. In terms of the kinetics data, there were, at best, small changes from the binary blend data except for the rate of phase separation. The rate of phase separation for the SBR5050 blend was slower than the binary blend but faster than the other two copolymers. To get a better understanding of the molecular weight and polydispersity, experiments should be done with higher molecular weight monodisperse copolymers. Finally, these results suggest that tailoring the copolymer structure and molecular weight are very important in affecting both the equilibrium and kinetic properties of a blend.

## Conclusion

The primary results provide information regarding the influence of an additive's structural properties on both the equilibrium and kinetics aspects of phase separation in modified polymer blends. From cloud point measurements, the symmetric additives (SBR5050 and SBB5050) stabilized the thermodynamic boundary to phase separation while the asymmetric random copolymer (SBR2080) destabilized the system. The block copolymer was the most effective at lowering the phase boundary temperature. In terms of the kinetics of spinodal decomposition, all of the additives slowed the growth of the intensity of scattering. The domain sizes of the blend with the SBB5050 additive started out equal in size to the binary blend; however, the domain

sizes grew at a slower rate than that of the binary blend. The domain sizes for the blend with the SBR5050 additive were virtually identical to the binary blend domain sizes. Last, the domain sizes for the blend with the SBR2080 additive started out and were at all times larger than the domain sizes of the binary blend. The intermediate scaling behavior is consistent with binary behavior except for that of the asymmetric copolymer. The symmetric diblock copolymer and the asymmetric random copolymer both caused significant deviations to the interface sharpness. Universal scaling curves worked well for all systems. Perhaps the most striking question is the behavior of the asymmetric blend where the phase boundary temperature goes up and rate of phase separation goes down.

These results illustrate the need to understand in more detail how an additive's structural properties influence and change the equilibrium properties of a binary blend and the kinetics of phase separation. Studying a different random copolymer compositions and well as other copolymer structures should be enlightening. In addition, small-angle neutron scattering (SANS) may hold promise in understanding the differences in these systems. The thermodynamic parameter,  $\chi$ , and the correlation length may be oppositely affected by the asymmetric additive compared to the symmetric additive. SANS experiments are being pursued to help answer these questions.

**Acknowledgment.** Support for this research is gratefully acknowledged from the William and Flora Hewlett Foundation Award of Research Corporation (C-3491), a National Science Foundation Research in Undergraduate Institutions Award (DMR-9705424), and a Regency Advancement Award (Pacific Lutheran University). D.A.W. acknowledges Brad Reppen and J. Chris Bock for their help in the construction of the light scattering instrumentation. Discussions with Dr. Steve Starkovich and Dr. Mark Dadmun are also gratefully acknowledged.

## References and Notes

- (1) *Polymer Blends*, Paul, D. R., Bucknall, C. B., Eds.; Wiley: New York, 1999.
- (2) *Polymer Alloys and Blends*, Utracki, L. A., Ed.; Hansen Publishers: Munich, 1989.
- (3) *Polymer Blends*, Paul, D. R., Newman, S., Eds.; Academic Press: New York, 1978.
- (4) Han, C. C. In *Molecular Conformation and Dynamics of Macromolecules in Condensed Systems*; Nagasawa, Ed.; Elsevier Science Pub: Amsterdam, 1988; p 223.
- (5) Hashimoto, T. *Phase Transitions* **1988**, 12, 47.
- (6) Freed, K. F.; Dudowicz, J. *Macromol. Symp.* **1996**, 112, 17.
- (7) Freed, K. F.; Dudowicz, J. *Pure Appl. Chem.* **1995**, 67, 969.
- (8) Reichart, G. C.; Graessley, W. W.; Register, R. A.; Krishnamoorti, R.; Lohse, D. J. *Macromolecules* **1997**, 30, 3363.
- (9) Curro, J. G.; Schweizer, K. S. *Polym. Mater. Sci. Eng.* **1990**, 62, 702.
- (10) Curro, J. G.; Schweizer, K. S. *Macromolecules* **1991**, 24, 6736.
- (11) Balsara, N. P.; Lin, C.; Hammouda, B. *Phys. Rev. Lett.* **1996**, 77, 3847.
- (12) Lohse, D. J. *Macromol. Chem.* **1992**, 3, 184.
- (13) Dai, C.-A.; Dair, B. J.; Dai, K. H.; Ober, C. K.; Karmer, E. J.; Hui, C.-Y.; Jelinski, L. W. *Phys. Rev. Lett.* **1994**, 73, 2472.
- (14) Dai, C.-A.; Dair, B. J.; Dai, K. H.; Ober, C. K.; Karmer, E. J.; Hui, C.-Y.; Jelinski, L. W. *Phys. Rev. Lett.* **1995**, 74, 2836.
- (15) Noolandi, J.; Shi, A.-C. *Phys. Rev. Lett.* **1995**, 74, 2836.
- (16) Balazs, A. C.; DeMeuse, M. T. *Macromolecules* **1989**, 22, 4260.
- (17) Lyatskaya, Y.; Balazs, A. C. *Macromolecules* **1996**, 29, 7581.
- (18) Lyatskaya, Y.; Gersappe, D.; Gross, N. A.; Balazs, A. C. *J. Phys. Chem.* **1996**, 100, 1449.
- (19) Dadmun, M. D. *Macromolecules* **1996**, 29, 3868.
- (20) Dadmun, M. D. *Mater. Res. Soc. Symp. Ser.* **1997**, 461, 123.

- (21) Dadmun, M.; Waldow, D. *Phys. Rev. E* **1999**, *60*, 4545.  
(22) Rigby, D.; Lin, J. L.; Roe, R. J. *Macromolecules* **1985**, *18*, 2269.  
(23) Roe, R.; Kuo, C. *Macromolecules* **1990**, *23*, 4635.  
(24) Park, D.; Roe, R. *Macromolecules* **1991**, *24*, 5324.  
(25) Sung, L.; Hess, D. B.; Jackson, C. L.; Han, C. C. *J. Polym. Res.* **1996**, *3*, 139.  
(26) (a) Hashimoto, T.; Izumitani, T. *Macromolecules* **1993**, *26*, 3631. (b) Hashimoto, T.; Izumitani, T. *Macromolecules* **1994**, *27*, 1744.  
(27) Takenaka, M.; Hashimoto, T. *Macromolecules* **1996**, *29*, 4134.  
(28) Cahn, J. W.; Hilliard, J. E. *J. Chem. Phys.* **1958**, *29*, 258.  
(29) Krause, S.; Lu Z.-H. *J. Polym. Sci., Polym. Phys. Ed.* **1981**, *19*, 1925.  
(30) Sato, T.; Han, C. C. *J. Chem. Phys.* **1988**, *88*, 2057.  
(31) Stein, R. S.; Keane, J. J. *J. Polym. Sci.* **1955**, *17*, 21.  
(32) Roe, R.; Kuo, C. *Macromolecules* **1990**, *23*, 4635.  
(33) Sung, L.; Han, C. C. *J. Polym. Sci., Polym. Phys.* **1995**, *33*, 2405.  
(34) Dudowicz, J.; Freed, K. F.; Douglas, J. F. *Macromolecules* **1995**, *28*, 2276.  
(35) Timmermans, J. *Z. Phys. Chem. (Munich)* **1907**, *58*, 129.  
(36) Hales, B. J.; Bertrand, G. L.; Hepler, L. G. *J. Phys. Chem.* **1966**, *70*, 3970.  
(37) Cohn, R. H.; Jacobs, D. T. *J. Chem. Phys.* **1984**, *80*, 856.  
(38) Hashimoto, T.; Itakura, M.; Shimidzu, N. *J. Chem. Phys.* **1986**, *85*, 6773.  
(39) Synder, J. L.; Meakin, P. *J. Polym. Sci., Polym. Symp.* **1985**, *73*, 217.  
(40) Porod, G. In *Small Angle X-Ray Scattering*; Glatter, O., Kratky, O., Eds.; Academic Press: New York, 1982; Chapter 2, p 17.  
(41) Rulund, W. *J. Appl. Crystallogr.* **1971**, *4*, 10.

MA992182R